JOURNAL OF SOLID STATE CHEMISTRY 103, 375–386 (1993)

Layered Perovskitic Structures in Pure and Doped $LaTiO_{3.5-x}$ and $SrNbO_{3.5-x}$

TIM WILLIAMS

CSIRO Division of Materials Science and Technology, Locked Bag 33, Clayton, Victoria 3168, Australia

FRANK LICHTENBERG,† DANIEL WIDMER, AND J. GEORG BEDNORZ

IBM Research Division, Zürich Research Laboratory, 8803 Rüschlikon, Switzerland

AND

ARMIN RELLER*

Institute for Inorganic and Applied Chemistry, University of Hamburg, Martin-Luther-King-Platz 6, D-2000 Hamburg 13, Germany

Received April 10, 1992; in revised form August 31, 1992; accepted September 2, 1992

The effect of careful control over metal and oxygen stoichiometry on the structures of various $M_{n+1}M'_{n+1}O_{3n+5}$ phases (M = La and/or Sr, M' = Ti and/or Nb) has been studied by transmission electron microscopy. In addition to the previously reported $n = 3$ and 4 layered phases and the $n = \infty$ parent perovskite, ordered and disordered intergrowth structures comprising the $n = 2$, 3, 4, and ∞ members have been characterized. The effects of *in situ* reduction in the electron microscope were studied.

1. Introduction

The titanates $La_2Ti_2O_7$ and $Nd_2Ti_2O_7$ (*1*) and the alkali-metal niobates such as $Sr_2Nb_2O_7$ (*2*) and the Ca analogue are isomorphous and have layered structures belonging to a homologous series, $M_{n+1}M'_{n+1}O_{3n+5}$, $0 \leq n \leq \infty$, derived from the perovskite archetype (*3*). Many of these fully oxidized, $n = 3$ materials $M_2M'_2O_7$ (= $M_4M'_4O_{14}$) are high transition-temperature ferroelectrics. By reduction of the $n = 3$ phases, $n = 4$ compounds are formed, e.g., $La_5Ti_5O_{17}$ and $Ca_5Nb_5O_{17}$, which are semiconductors between room temperature and 4 K and have similar layered structures (*4*, *5*). The parent $n = \infty$ structure of the $LaTiO_x$ compounds, the orthorhombic perovskite $LaTiO_{3.0}$, is a weakly ferromagnetic semiconductor (*4*, *6–8*). Compounds with these

* To whom correspondence should be addressed.

† Present address: VARTA Batterie AG, R&D Center, 6233 Kelkheim, Germany.

0022-4596/93 $5.00

structures are therefore of considerable interest to the solid state chemist, as both the structure and the physical properties are determined largely by the oxygen stoichiometry and hence the transition metal electronic structure (*4, 5*).

Compared with the profusion of homologous {100} perovskite layered structures $M_{n+2}M'_{n+1}O_{3n+4}$, $0 \leq n \leq \infty$ (exemplified by the Ruddlesden–Popper phases Sr_2TiO_4, $Sr_3Ti_2O_7$ and, with some modifications, by very many of the high-T_c superconductors based on copper oxide perovskitic structural elements), surprisingly few compounds have been reported with these {110} perovskite structures. Although the number of perovskitic slabs per layer repeat unit (1 or 2 in the integral n members) and the unit cell symmetries (orthorhombic or monoclinic at room temperature in most cases) vary between homologues, their structures can be idealized to {110} slabs of the perovskite structure of different thicknesses (*9*). The $n = 0$ and 2 members of this family have not been previously reported, but a range of $n = 1$ ABF_4 compounds (A = Ba, Sr; B = Mg, Mn, Fe, Co, Ni, Zn) (*10–12*) and the quaternary oxyfluoride $NaNbO_2F_2$ (*13*) are known. These compose single crenellated BX_6 octahedral layers bounded by a zigzag layer of A cations. The A cation-deficient structure of $Bi_4Nb_5O_{18}F$ (*14*) can be described as the $n = 1$ structure $BiNb(O,F)_4$, with an additional row of $[NbO_6]$ octahedra in alternate layers. The perovskitic A sites in the thicker $[BiNb_2O_x]$ octahedral layers are empty, but otherwise these alternate thicker layers have the $n = 2$ structure type. This is a perfectly ordered intergrowth phase of $n = 1$ with A-deficient $n = 2$. $La_2Ti_2O_7$ ($= La_4Ti_4O_{14}$) and $La_5Ti_5O_{17}$ typify the most well-characterized, $n = 3$ and $n = 4$ materials in the family, respectively. In the $LaTiO_x$ system, only the $n = 3$, 4, and $n = \infty$ members exist as single phases (*4, 9*). Other workers have reported more or less disordered phases with n higher than 4 in (mainly) transmission electron microscope (TEM) studies (*15, 16*), for example a lattice fringe TEM image of $n = 5$, $(Na_2Ca_4)Nb_6O_{20}$ ordered over a large region of crystal in Ref. (*15*), but 4 seems to be the upper n limit for the truly ordered homologues in the systems studied to date. As well as the occasional observation of lamellae of material with $n >$ 4, TEM lattice fringe studies of Ca–Nb–O (*17*) and high-resolution imaging of Sr $NbO_{3.45}$ (*5*) revealed quite well-ordered intergrowth of the $n = 3$ and 4 material, giving $n = 3.5$.

It was thus of interest to us, as a part of a continuing study of these layered titanates and niobates, to attempt the preparation and structural characterization of new members of this homologous family. We were particularly interested in determining whether careful control of oxygen stoichiometry alone during the synthetic procedure was sufficient to form well-ordered intergrowth phases between $n = 3$ and 4, and n members between 4 and the perovskite. We report below on some results of this study, mainly by transmission electron microscopy (TEM), and also on attempts to prepare a single oxide phase with the missing $n = 2$ structure type by partial substitution of Nb^{5+} for Ti^{4+}. The studies reported here concern primarily the ternary La–Ti–O and quaternary La–(Ti,Nb)–O and (La,Sr)–Nb–O systems.

2. Experimental

All the samples were prepared by solid state reaction in argon or air involving appropriate mixtures of high-purity metals, binary oxides, and carbonates followed by crystal growth using a zone-melting method in argon or air (*4, 5, 9*). A wide range of compositions were prepared and only some of these are discussed here. The experimental technique used for $Sr_{1-y}La_yNbO_x$ has been described previously (*5*). We attempted to prepare an $n = 2$ phase by adopt-

ing a mixed B cation system. With fully oxidized metals and using La as the A cation, the B cation valence for a phase $La_3(B)_3O_{11}$ with the $n = 2$ structure is $+4\frac{1}{3}$. We used a mixture of $2Ti^{4+} + Nb^{5+}$ in order to achieve this B valence. Thermogravimetric analysis (TGA) was done on all the as-melted samples in order to determine the degree of reduction, as described previously (*4, 5, 9*), and the oxygen compositions for the products reported below were those determined experimentally. These oxygen stoichiometries are relevant for the bulk products; i.e., they may result from domain structures adopting different, but structurally well-defined fragments.

Samples were examined in a Siemens D 500 diffractometer using $CuK\alpha_1$ radiation to ascertain the presence or absence of impurities such as unreacted La_2O_3 and unwanted ternary products, but the powder diffraction data were not usually used further. It was found that indexing the patterns of the larger unit-cell phases unambiguously was extremely difficult, due to mixed-phase products, the strong perovskitic subcells, and the qualitative similarities of patterns from the different homologues. The unit-cell information given below was therefore obtained by electron diffraction.

TEM specimens were prepared by crushing the products under ethanol in an agate mortar and collecting some of the resulting suspension on a holey-carbon-coated copper mesh. These samples were examined mainly in the NAMAC[1]/CSIRO Philips CM30 equipped with a TWIN lens (spherical aberration coefficient $C_s = 2$ mm) and double-tilt holders, operated at 300 kV. The $La_3Ti_2NbO_{11}$ sample was also examined in the ETH Zürich Philips SUPER-TWIN CM 30 ($C_s = 1.2$ mm). Both machines were also equipped with energy-dispersive X-ray (EDX) spectrometers for elemental analysis.

[1] National Advanced Materials Analytical Centre, Locked Bag 33, Clayton 3168, Victoria 3168, Australia.

3. Results and Discussion

Although in most cases images and selected-area diffraction patterns (SADP) were obtained from a wide variety of zone axis orientations, we consider in detail only the results from the [100] zones below. We found that this zone provided the most useful information regarding the layer structures, as the fragments were usually much thinner than those from the [010] or other zone-axes. As in the phases $La_2Ti_2O_7$ and $La_5Ti_5O_{17}$ (*9*), the angle β was found to be $\neq 90°$ in the intergrowths of these phases also; as nearly as we could determine α and γ are 90°. We therefore deduce that the intergrowths, like the parent materials, are of no higher than monoclinic symmetry in the La–Ti–O system. The unit cells thus have approximately the same a (~7.8 Å) and b (~5.5 Å) parameters in all cases: the layer-repeat, c parameters were estimated from the images and diffraction patterns. The Sr–Nb–O $n = 3$ and 4 members, on the other hand, are of orthorhombic symmetry (*2, 5*) and this appears to be the case for the intergrowths described below. These phases have a halved a repeat (~3.9 Å) and the same b (~5.5 Å) as the La–Ti–O compounds. But accurate determination of the cell angles and symmetries for all these very-long-period intergrowths is somewhat difficult and is the subject of continuing work.

3.1. La-(Ti,Nb)-O System

In an attempt to prepare a phase with the $n = 2$ structure, a sample of nominal composition $La_3Ti_2NbO_{11}$ was zone-melted in air. However, due to incongruent melting, the product obtained was polycrystalline. Powder X-ray examination of the light straw-colored, insulating product showed the presence of strong lines attributable to the phase $LaNbO_4$, which has the fergusonite structure, a monoclinic distortion of the scheelite $CaWO_4$ structure type (*18*). The remainder of the pattern was qualitatively

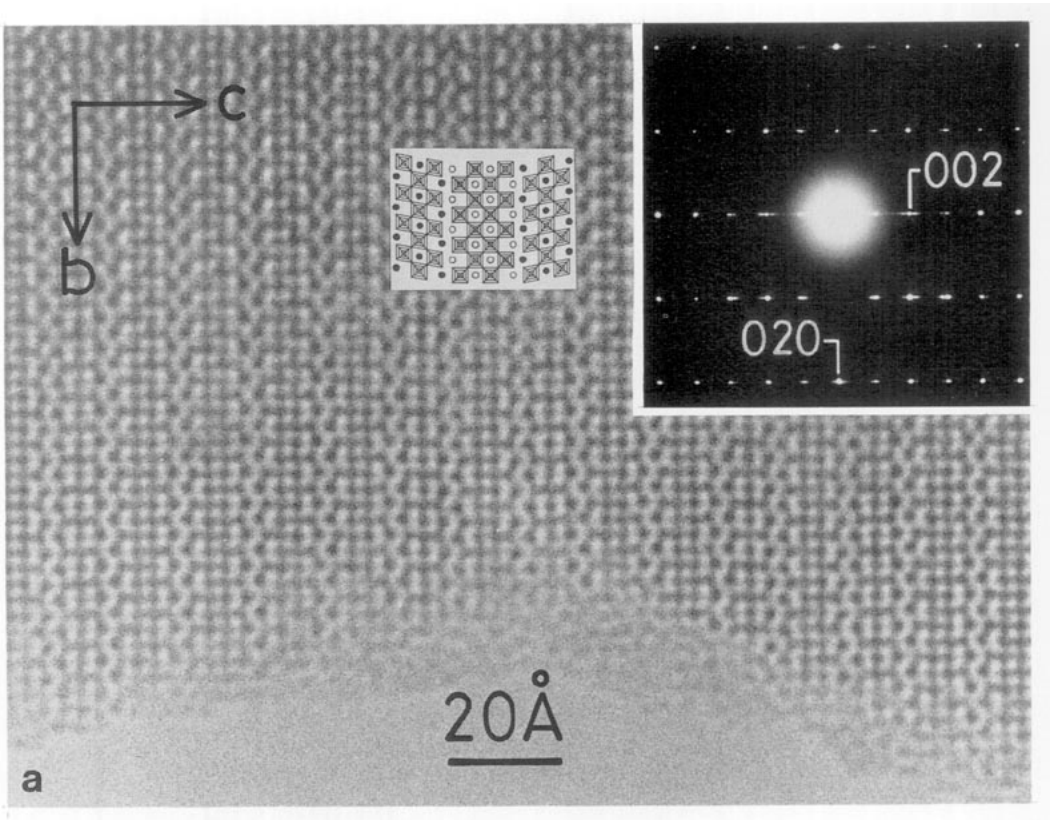

FIG. 1a. HRTEM image and corresponding SADP (inset) from a crystal of $La_3(Ti,Nb)_3O_{11}$. This crystal contains a high density of layers with the $n = 2$ structure type disordered in an $n = 3$ matrix. Inset in the image is a structure drawing which shows two $n = 2$ and one $n = 3$ layers which correspond to the underlying image. At the thin edge of the crystal, the cation positions are clearly resolved as dark spots of two sizes and the interlayer boundary is visible as a zigzag band between the layers. The SADP shows some streaking of $00l$ reflections but no evidence for ordering.

similar to patterns from $La_2Ti_2O_7$, indicating that the sample also comprised a layered phase. TEM, combined with EDX analyses, showed that the fergusonite-like phase constituted the majority of the sample (50 ~ 75%), but that the remainder was a layered perovskite-related material. Figure 1a shows a high-resolution transmission electron microscope (HRTEM) image from the latter together with the corresponding SADP. From this and other images and SADPs not shown, the orientation in Figure 1a was deduced to be the [100] zone of the $La_2Ti_2O_7$ structure, parallel with the ~7.8 Å axis of the cell. The image shows a characteristically layered structure, comprising repeat lamellae of two sorts. The first, and the majority in all of the crystals examined, are ~13 Å thick, which corresponds to the $n = 3$ structure type of $La_2Ti_2O_7$. As may be seen in the inset structure drawing in the figure, these $n = 3$ layers are four corner-sharing TiO_6 octahedra wide with La in the usual perovskitic A sites as well as the interlayer region. The second, minority layers are apparently thinner by one octahedral unit, and thus have the $n = 2$ structure type. We estimate from EDX analyses that

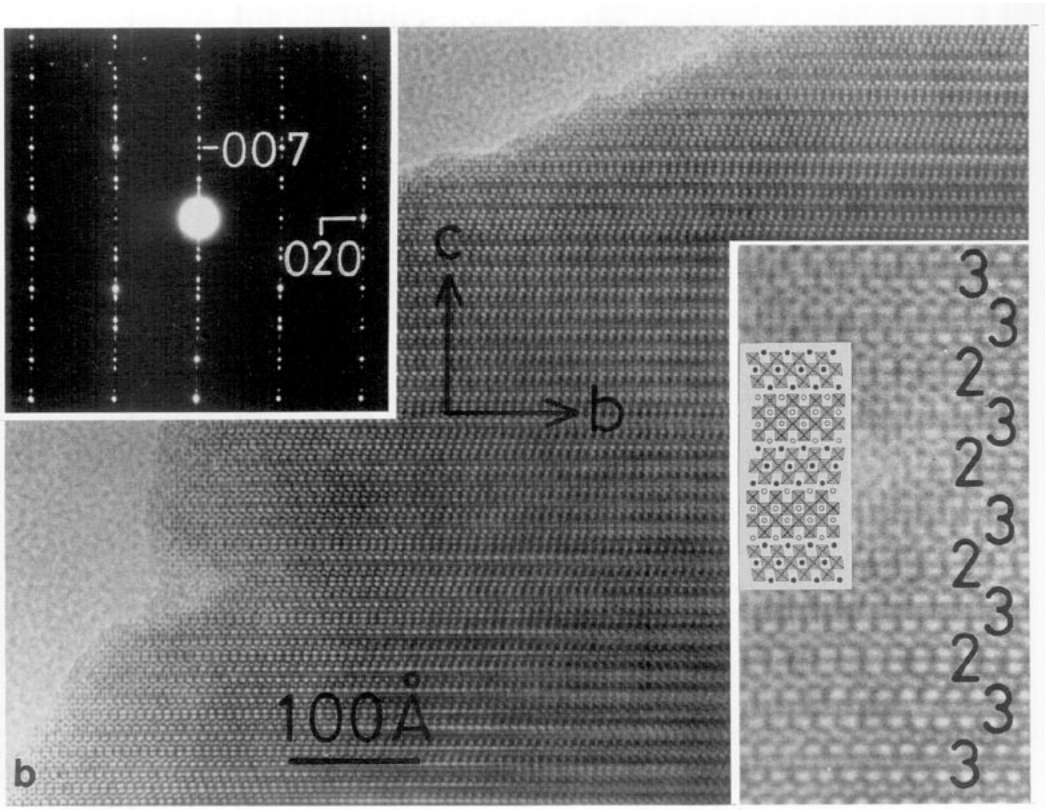

FIG. 1b. HRTEM image from an $La_3(Ti,Nb)_3O_{11}$ crystal which shows (in the lower left part) partial ordering of $n = 2$ and 3 layer types. This is confirmed by the SADP (inset) which shows sharp superlattice reflections corresponding to a c repeat of ~46 Å. The b repeat remains that of the matrix $La_2Ti_2O_7$ at ~5.5 Å. The enlarged inset is of the edge of this crystal, with the structure drawing overlaid for comparison.

-crystals such as that shown in Fig. 1a were of approximate composition $La_3(Ti_{0.8}Nb_{0.2})_3O_{11}$, somewhat Ti-rich compared with the starting composition. The excess $LaNbO_4$ phase apparently forms freely under these preparation conditions and reduces the Nb/Ti ratio in the layered perovskitic phase, encouraging the preferential formation of the $n = 3$ phase. Figure 1b shows a crystal from this sample showing good ordering of the $n = 2$ and 3 layer types. The inset zone-axis diffraction pattern (shown enlarged in Fig. 4a) suggests a layer repeat of ~46 Å, which results from the intergrowth of ~13 Å thick $n = 3$ with ~10 Å thick $n = 2$, repeating every second pair of layers. This was the only crystal out of very many examined which showed any extended ordering of the layers, and the corresponding EDX analysis suggests a Nb/Ti ratio of about 1/4.4. As a comparison, 1 : 1 ordering of $n = 3$ $La_4Ti_4O_{14}$ and hypothetical $n = 2$ $La_3Ti_2NbO_{11}$ yields a ratio of Nb/Ti = 1/6. The Nb-rich observed composition may be due to some replacement of Ti by Nb in the $n = 3$ layers.

3.2. *$LaTiO_x$ System*

We have reported elsewhere (*4*, *9*) on the stability of the $n = 4$ phase $La_5Ti_5O_{17}$ against

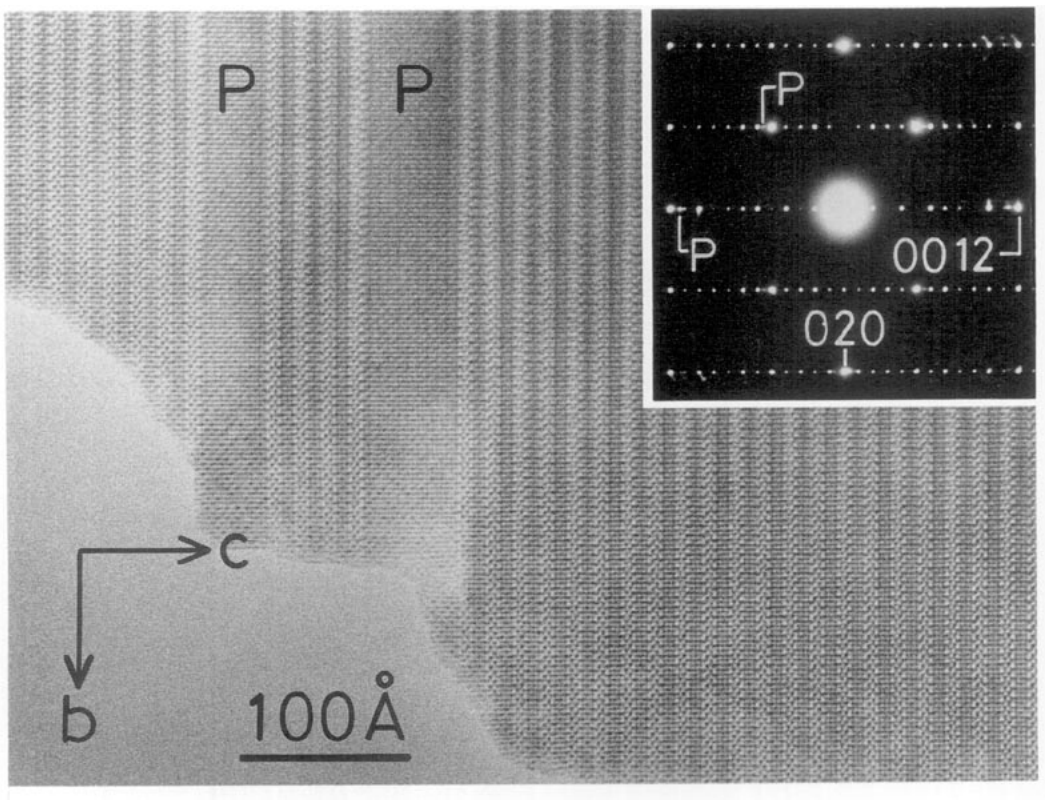

FIG. 2. HRTEM image and SADP from a sample of composition $LaTiO_{3.22}$. As well as the $n = 4$ phase, appreciable quantities of perovskite are present as broad, intergrowth bands: two such bands are indicated by **P** in the image. The perovskite intergrows readily with the matrix layered material in bands of up to a few 100 Å in thickness. The perovskite bands generate additional reflections **P** in the SADP.

reduction and for compositions of $LaTiO_x$ with $3.40 \leq x \leq 3.42$, an apparently single phase $n = 4$ product forms. Powder X-ray diffraction patterns from preparations with $x < 3.40$ contain, in addition to peaks from $La_5Ti_5O_{17}$, increasing intensity in the positions expected for the orthorhombic $LaTiO_3$ archetype. However, the positions and intensities of peaks attributable to the layered $n = 4$ phase do not alter sufficiently to suggest that a different layered phase is forming. Down to $x = 3.29$ only $n = 4$ phase, and very rarely perovskite, fragments can be detected in the TEM. In samples with $3.20 < x \leq 3.28$, we frequently observed the coexistence of $n = 4$ and the perovskite in the form of disordered intergrowths, a typical example of which is shown in the TEM image of Fig. 2, a fragment from a preparation with $x = 3.22$. Therefore we assume that in the ternary system n members above 4 are not stable under these preparation conditions.

Several preparations were made with compositions between $n = 4$ and $n = 3$ ($3.42 < x < 3.50$), the composition being controlled by careful variation of the TiO_2 to TiO or Ti ratio in the starting material. Although TGA of the product showed that a small uptake of oxygen invariably occurred,

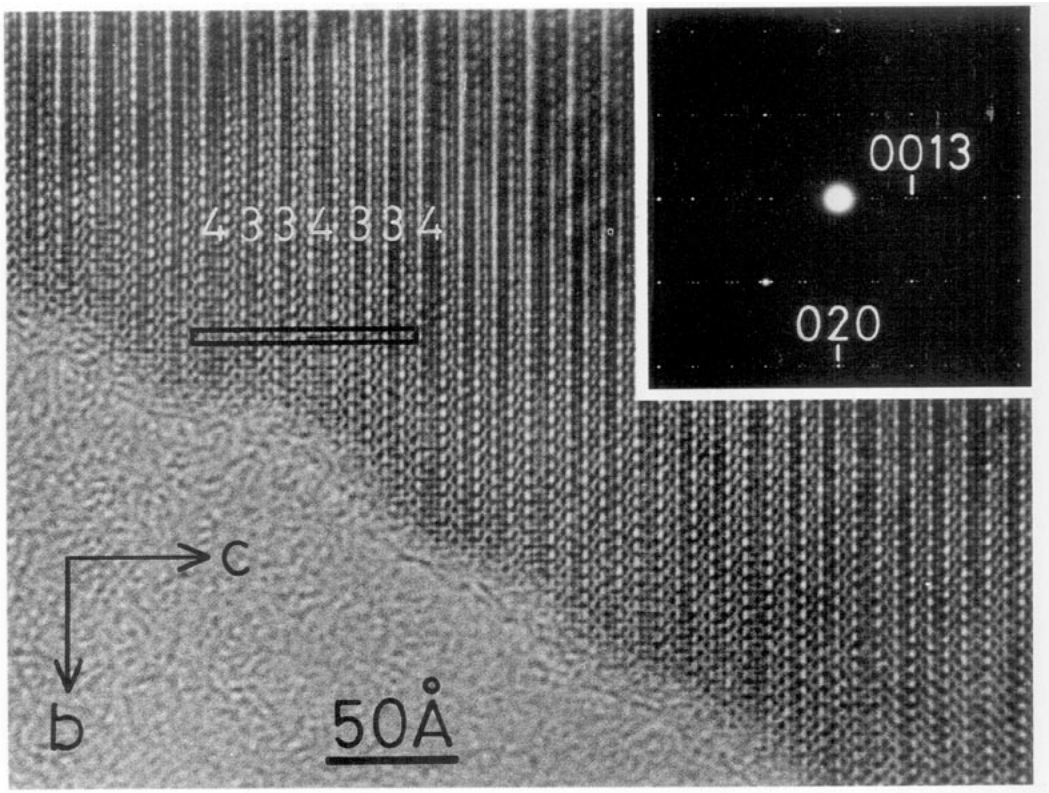

FIG. 3. A sample of composition $LaTiO_{3.46}$ comprised an almost perfectly ordered intergrowth of the $n = 3$ and 4 homologues, in the sequence –[3–3–4–3–3–4]–. The resulting unit cell, $a = 7.8$ Å, $b = 5.5$ Å, $c = 85$ Å, is outlined on the image. Sharp supercell reflections in the SADP (inset) confirm the perfection of the ordering.

we could prepare samples with compositions of $3.42 < x < 3.50$ as determined from TGA. X-ray diffraction patterns from these materials suggested largely similar structures to the $n = 4$ ($3.40 \leq x \leq 3.42$) phase, but with significantly altered positions and intensities for some peaks. Fragments from these samples were examined in the TEM in several zone axis orientations. Figure 3 shows a crystal from a sample with composition $LaTiO_{3.46}$ in the [100] orientation. This image shows a region containing well-ordered intergrowth of single ~16-Å-wide $n = 4$ lamellae with pairs of ~13-Å-wide $n = 3$ lamellae. Although not visible in this image, the ordering was occasionally disturbed by either 1 less or 1 more $n = 3$ lamella, but apparently maintaining the overall composition. Electron diffraction patterns from this material (inset in Fig. 3 and enlarged in Fig. 4c) suggest a layering (c) repeat of ~85 Å, which corresponds to a repeat unit consisting of $2 \times [2 \times (n = 3) + (n = 4)]$. Well-ordered regions of this crystal are thus of composition $LaTiO_{3.47}$ if the maximal oxygen stoichiometries, $x = 3.42$ and 3.50, respectively, are assumed for the $n = 4$ and 3 layer types. The origin of the doubled c repeat is revealed by the TEM images, and is due to the displacement of

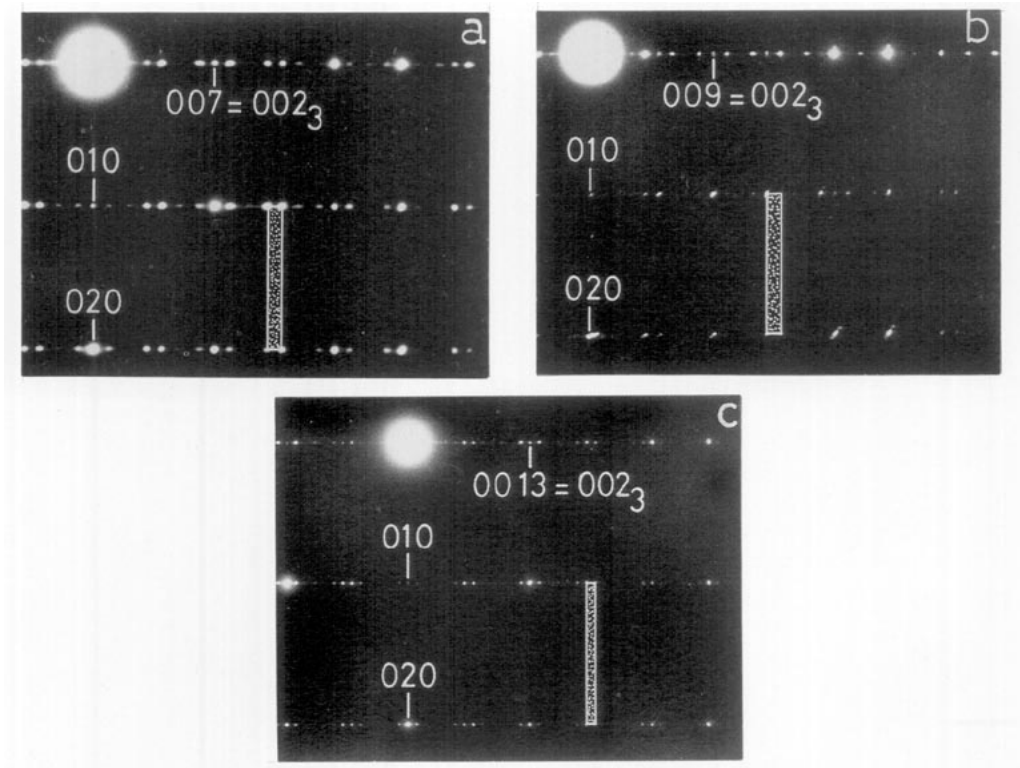

FIG. 4. Enlargements of [100] zone-axis SADPs from (a) $La_3(Ti,Nb)_3O_{11}$ (Fig. 1b), (b) $SrNbO_{3.45}$ (Fig. 5), and (c) $LaTiO_{3.46}$ (Fig. 3), comparing the three types of ordered layer superstructures in these materials. In each pattern the supercell is stippled and the reflections are indexed according to this supercell; also the position of the 002 reflection from the $n = 3$ structure type is indicated. There are no systematic absences of reflections from these three large structures.

alternate $n = 4$ layers by $b/2$, a stacking requisite of the symmetrical, five-cation-layers-thick $n = 4$ layers.

3.3. Sr–La–Nb–O System

Results obtained from the Sr–Nb–O system are comparable with those from the La–Ti–O system over a large range of oxygen composition. Reduction of the ferroelectric phase $Sr_2Nb_2O_7 = SrNbO_{3.5}$ results in the formation, at the composition $SrNbO_x$, with $3.40 \leq x \leq 3.42$, of an $n = 4$ layered phase which is isostructural with $LaTiO_{3.4}$ (*5*) but on further reduction our present XRD and TEM studies indicate the formation of an unknown and probably nonperovskitic phase rather than the perovskite parent. Between $x = 3.42$ and 3.50, $SrNbO_x$ forms two kinds of well-ordered intergrowths of the $n = 3$ and $n = 4$ structures. Figure 5 is a high-resolution TEM image from a sample with nominal composition $SrNbO_{3.45}$, which shows perfectly-ordered alternation of individual $n = 3$ and $n = 4$ layer types. However, the electron diffraction pattern (inset in Fig. 5 and enlarged in Fig. 4b) reveals the repeat in the layer-stacking direction **c** to be about 59 Å, which suggests that the basic layer-pair sequence repeats twice per unit cell, as we observed for the $LaTiO_{3.46}$ sample described above, giving –[3–4–3–4]– stacking. By reference to the

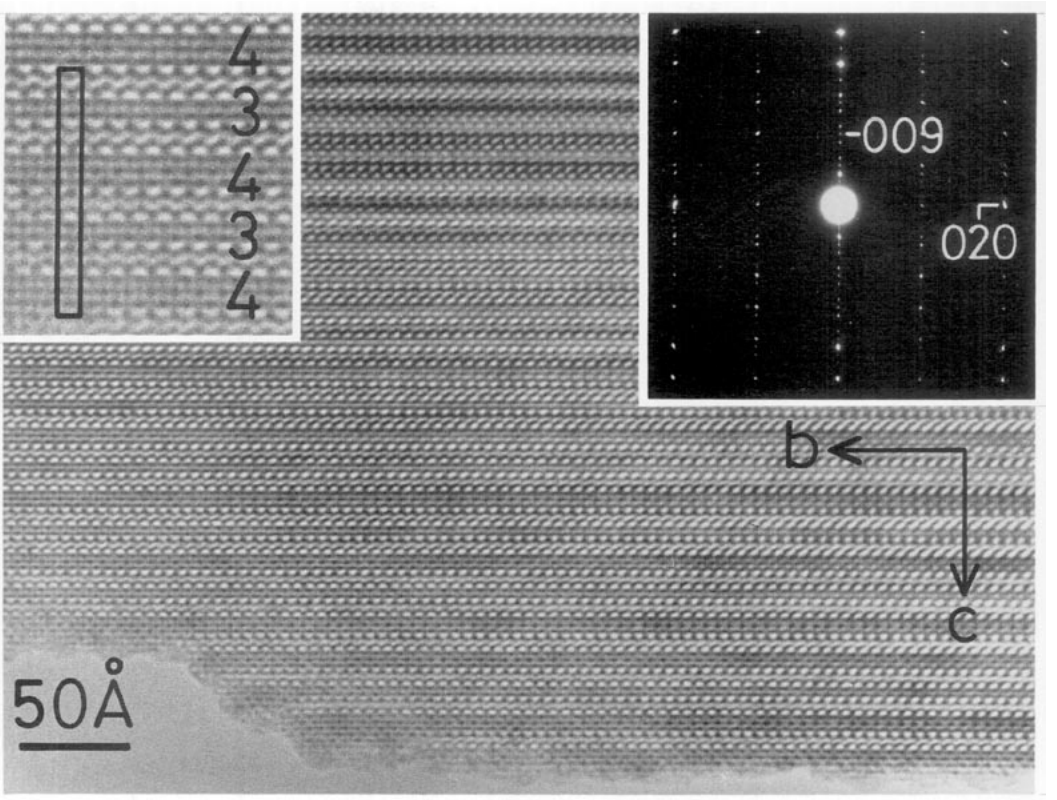

FIG. 5. HRTEM [100] zone-axis image from a fragment of $SrNbO_{3.45}$ showing perfectly ordered intergrowth of $n = 3$ and 4 layers. The inset enlargement of the image shows the unit cell, which comprises four layers; the SADP is indexed according to this cell. Note that at the extreme edge of this crystal some reduction has started to take place, resulting in thickening of the layers.

inset enlargement in Figure 4, the origin of this doubling is revealed to be the **b**/2 shift of alternate $n = 4$ layers, as is the case in the parent $n = 4$ structure of $La_5Ti_5O_{17}$ (*9*) and also both the –[3–3–4–3–3–4]– intergrowth structure of $LaTiO_{3.46}$ (Fig. 3) and the partly-ordered –[2–3–2–3]– intergrowths in Fig. 1b. Although more easily seen in Fig. 1a and the inset enlargement of Fig. 5, the even-numbered n layers of this structural type, either in the pure phase (for $n = 4$) or where they occur as intergrowths, also show a small amount of "canting," the canting being in opposite directions in alternate layers. Figure 6 illustrates schematically these three types of ordered intergrowth structures, with the "canting" of the even n layers exaggerated slightly for clarity.

Figure 7 shows a TEM image from a crystal of the sample $Sr_{0.8}La_{0.2}NbO_{3.51}$; the fully oxidized composition would be $Sr_{0.8}La_{0.2}NbO_{3.60}$. This sample was black in color and semiconducting between room temperature and 4 K. Although XRD examination of the product suggested a pure $n = 3$ phase, the TEM images from this material showed a low, but easily detected density of $n = 4$ lamellae intergrown in the $n = 3$ matrix. These $n = 4$ layers presumably account for both the color and the electrical properties of the sample. Three quite closely spaced $n = 4$ layers are indicated in Fig. 7.

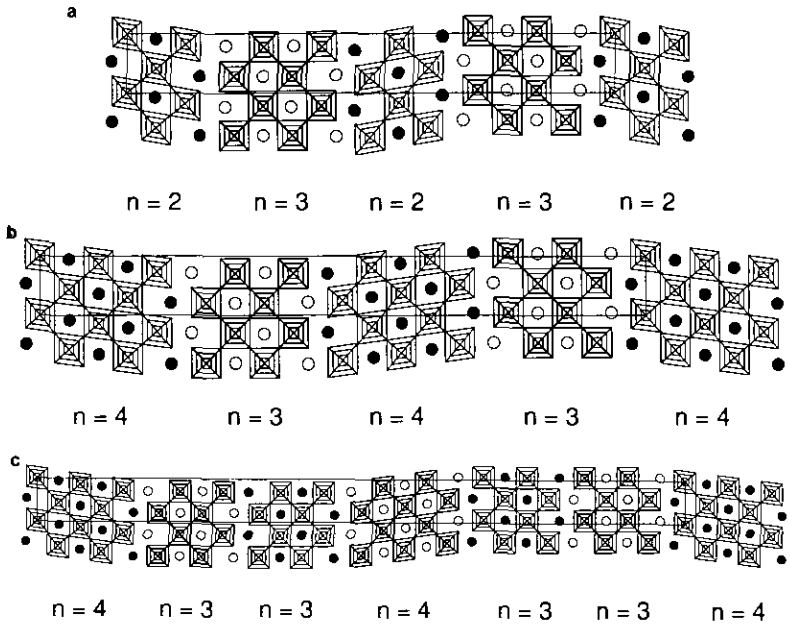

FIG. 6. Schematic drawings of the observed ordered intergrowth structures projected down [100]. (a) *The –[2–3–2–3]– type found in* $La_3(Ti,Nb)_5O_{11}$. (b) *The –[3–4–3–4]– type found in* $SrNbO_{3.45}$. (c) The –[3–3–4–3–3–4]– type found in $LaTiO_{3.46}$. The canting of the even-numbered layers has been exaggerated for clarity and the unit cells are outlined. Large filled and open circles: *A* site cations (La, Sr); ruled polyhedra: *B* site (Ti,Nb) metal–oxygen octahedra. Alternate layers are displaced by half an octahedron height in the [100] direction.

Although the La–Ti–O materials were always completely stable in the electron microscope, the Sr–Nb–O samples were quite rapidly reduced by irradiation with 300 kV electrons in the microscope vacuum. This offered an opportunity to study the further reduction of the $n = 3$ and $n = 4$ phases in this system, as only the $n = 4$ phase could be prepared as a bulk material. Figure 8 shows two images from a crystal of the same $Sr_{0.8}La_{0.2}NbO_{3.51}$ sample as Fig. 7: the main part of the figure shows the later state of the crystal after irradiation, with a band (arrowed "2") about 320 Å long of thick, perovskite-like structure formed by the reduction of two adjacent $n = 3$ and $n = 4$ lamellae. Inset above is an image showing the state of the crystal about 15 seconds

FIG. 7. [100] zone-axis image and SADP from $Sr_{0.8}La_{0.2}Nb_{03.51}$ showing the occasional $n = 4$ layers (3 of which are arrowed) occurring from reduction of the $n = 3$ matrix. Fully oxidized material would have the composition $Sr_{0.8}La_{0.2}NbO_{3.60}$.

FIG. 8. The effects of *in situ* reduction of these materials are clearly illustrated in these HRTEM images of $Sr_{0.8}La_{0.2}Nb_{03.51}$. Approximately 15 sec elapsed between the two photographs, during which time a band of $n = 8$ material formed from adjacent $n = 3$ and 4 layers has advanced a further ~120 Å into the crystal from 1 to 2. The reduction process taking place is curiously similar to the "zipper" fastener, as adjacent layers are moving both closer together, eliminating oxygens in the interlayer region, and also slightly up (or down) in the [100] direction. Eventually the entire region under observation is transformed to material of near-perovskite composition but highly strained and disordered.

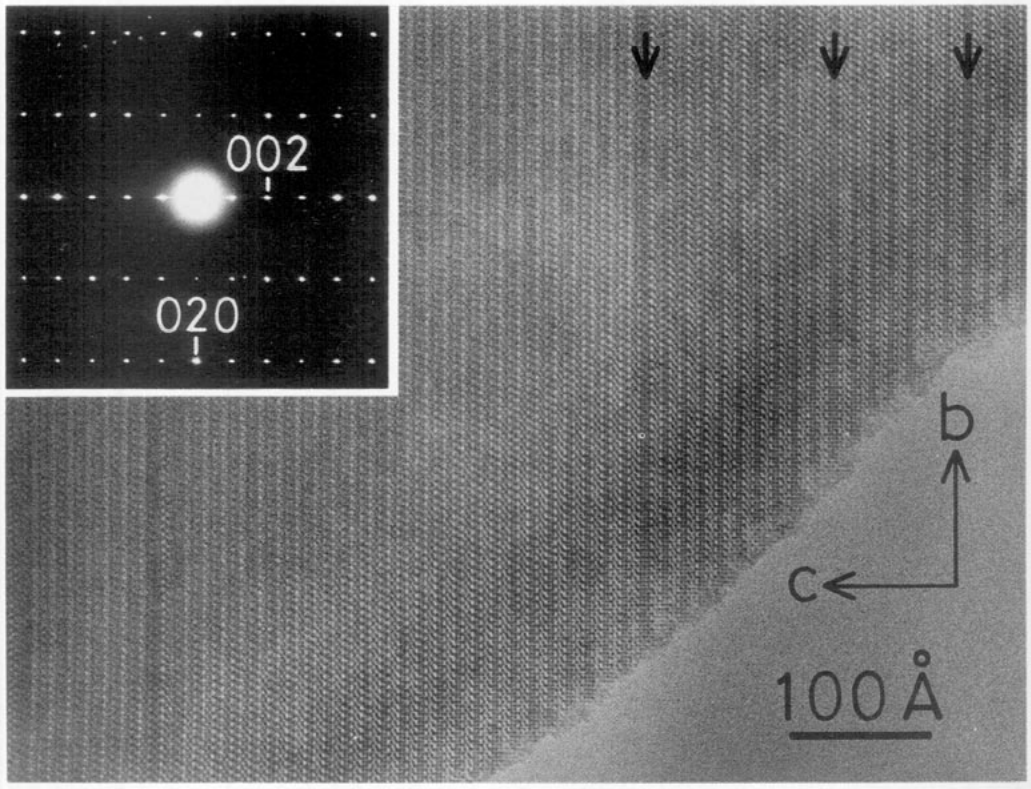

7

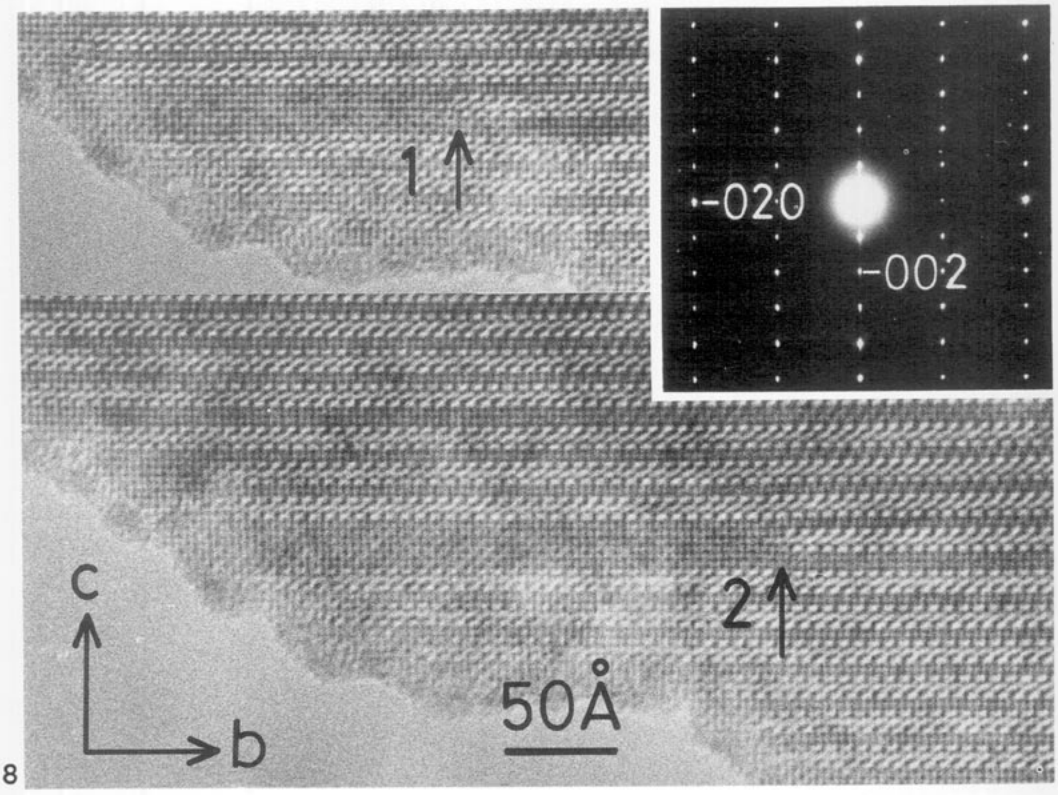

8

earlier, and the reduced band (1) has here only advanced about 200 Å from the crystal edge, where the in-beam reduction process always initiates. Reduction in this material is not limited to regions containing $n = 4$ layers, as there is a second reduced band beginning to attack the crystal immediately above the main one, comprising two $n = 3$ layers. Also visible in these images is the marked contraction of the layers in the **c** direction after reduction, giving the general appearance of a "zipper" advancing into the crystal. This most easily seen by viewing along the layers. Eventual formation of extensive but highly distorted perovskite islands occurs after lengthy irradiation.

4. Conclusions

Our present results show that preparation of perfectly ordered intergrowth phases comprising the homologous $n = 3$ and 4 layered structure types in these transition-metal oxide systems can be achieved by zone-melting under controlled conditions, and that transmission electron microscopy combined with accurate thermal analysis can usefully elucidate the structures formed. The ordered intergrowths have, in some cases, exceptionally long unit-cell repeats which in combination with the pronounced subcells would hinder X-ray structure examination. By control of the perovskite *B* cation stoichiometry it was possible to produce partially ordered intergrowth of the first $n = 2$ member of this homologous series in an $n = 3$ matrix, in the La–(Ti,Nb)–O system. We have been unable to produce *n* members between 4 and ∞ except as broad layers of near perovskite composition ($\sim O_{3.0}$) in nominally $n = 4$ matrices.

5. Acknowledgments

Tim Williams thanks Professor H. R. Oswald, University of Zürich, for his hospitality and acknowledges the financial support of the Swiss National Foundation for Science under project NF 2.772-0.87. We are grateful to Professor G. Kostorz, ETH Zürich, for his support and provision of time on the ETH Zürich CM 30 microscope. We are also indebted to R. Wessiken and P. Schwander (ETH Zürich), B. Spring (University of Zürich), P. Miller (NAMAC), and M. Fergus (CSIRO) for technical assistance.

6. References

1. M. Gasperin, *Acta Crystallogr. Sect. B* **31,** 2129 (1975).
2. F. Marumo, T. Kawamura, and M. Kimura, *Acta Crystallogr. Sect. B* **31,** 1912 (1975).
3. R. J. D. Tilley, *in* "Chemical Physics of Solids and their Surfaces" (M. W. Roberts and J. M. Thomas, Eds.), Chap. 6, p. 121, Royal Soc. of Chem. Great Britain (1980).
4. F. Lichtenberg, D. Widmer, G. Bednorz, T. Williams, and A. Reller, *Z. Phys. B* **82,** 211 (1991).
5. F. Lichtenberg, T. Williams, A. Reller, D. Widmer, and J. G. Bednorz, *Z. Phys. B* **84,** 369 (1991).
6. D. A. MacLean and J. E. Greedan, *Inorg. Chem.* **20,** 1025 (1981).
7. J. P. Goral and J. E. Greedan, *Magn. Mater.* **37,** 315 (1983).
8. Y. Maeno, S. Awaji, H. Matsumoto, and T. Fujita, *in* "Proceedings of the 19th International Conference on Low-Temperature Physics, Sussex, 1990."
9. T. Williams, H. Schmalle, A. Reller, F. Lichtenberg, D. Widmer, and J. G. Bednorz, *J. Solid State Chem.* **93,** 534 (1991).
10. M. Eibschütz and H. J. Guggenheim, *Solid State Commun.* **6,** 737 (1968).
11. H. G. von Schnering and P. Bleckmann, *Naturwissenschaften* **55,** Heft 7, 342 (1968).
12. E. T. Keve, S. C. Abrahams, and J. L. Bernstein, *J. Chem. Phys.* **51,** 4928 (1969).
13. S. Andersson and J. Galy, *Acta Crystallogr. Sect. B* **25,** 847 (1969).
14. L. Kihlborg, M. Sundberg, and Ö. Sävborg, *Ultramicroscopy* **18,** 191 (1985).
15. R. Portier, M. Fayard, A. Carpy, and J. Galy, *Mater. Res. Bull.* **9,** 371 (1974).
16. M. Nanot, Queyroux, F. and J.-C. Gilles, *C.R. Acad. Sci. Paris. Ser. C* **277,** 505 (1973).
17. M. Hervieu, F. Studer, and B. Raveau, *Solid State Chem.* **22,** 273 (1977).
18. S. Tsunekawa and H. Takei, *Phys. Status Solidi A* **50,** 695 (1978).